Differential signaling networks of Bcr-Abl p210 and p190 kinases in leukemia cells defined by functional proteomics

Running title: **Differential signaling of Bcr-Abl p210 and p190**

Sina Reckel[1], Romain Hamelin[2], Sandrine Georgeon[1], Florence Armand[2], Qinfang Jolliet[2], Diego Chiappe[2], Marc Moniatte[2] and Oliver Hantschel[1,3,*]

[1] Swiss Institute for Experimental Cancer Research (ISREC), School of Life Sciences, École polytechnique fédérale de Lausanne (EPFL), 1015 Lausanne, Switzerland

[2] Proteomics Core Facility, School of Life Sciences, École polytechnique fédérale de Lausanne (EPFL), 1015 Lausanne, Switzerland

[3] ISREC Foundation Chair in Translational Oncology

*Correspondence and requests for materials should be addressed to O.H. (email: oliver.hantschel@epfl.ch).

Abstract

The two major isoforms of the oncogenic Bcr-Abl tyrosine kinase, p210 and p190, are expressed upon the Philadelphia chromosome translocation. p210 is the hallmark of chronic myelogenous leukemia, whereas p190 occurs in the majority of B-cell acute lymphoblastic leukemia. Differences in protein interactions and activated signaling pathways that may be associated with the different diseases driven by p210 and p190 are unknown. We have performed a quantitative comparative proteomics study of p210 and p190. Strong differences in the interactome and tyrosine phosphoproteome were found and validated. Whereas the AP2 adaptor complex that regulates clathrin-mediated endocytosis interacts preferentially with p190, the phosphatase Sts1 is enriched with p210. Stronger activation of the Stat5 transcription factor and the Erk1/2 kinases is observed with p210, whereas Lyn kinase is activated by p190. Our findings provide a more coherent understanding of Bcr-Abl signaling, mechanisms of leukemic transformation, resulting disease pathobiology and responses to kinase inhibitors.

Introduction

The Bcr-Abl kinase and its inhibitors (imatinib and successors) are a paradigm for targeted cancer therapy[1]. Bcr-Abl is a constitutively active tyrosine kinase, expressed by the Philadelphia (Ph) chromosome. It is formed upon the t(9;22) reciprocal translocation that fuses the breakpoint cluster region (BCR) gene with the Abelson tyrosine kinase (ABL1)[2]. Depending on the translocation breakpoint in BCR, different Bcr-Abl protein isoforms are expressed, which all contain exons 2-11 of the ABL1 gene, but differ in the length of their BCR component[3]. The most common Bcr-Abl isoforms are p210 and p190 (alternatively named: p185). p190 is 501 amino acids, i.e. ~25%, shorter than p210 because it lacks a DH-PH domain unit; otherwise p210 and p190 have an identical sequence and domain organization (Fig. 1a)[4].

The expression of p210 is the molecular hallmark of chronic myelogenous leukemia (CML)[3]. The Ph-chromosome is also present in 20-30% of adult B-cell acute lymphoblastic leukemias (B-ALL), where approximately 1/4 of these patients express p210 and approximately 3/4 express p190 Bcr-Abl[3]. Treating CML patients with the Bcr-Abl tyrosine kinase inhibitor (TKI) imatinib leads to durable remissions in most patients and the survival of those patients is not different from that of the general population[5]. In contrast, in Ph-positive B-ALL, relapse and TKI resistance are frequent, and overall survival is still dramatically low, despite the increased remission rates and survival that can be achieved with Bcr-Abl TKIs[6,7].

p210 is the sole oncogenic driver that is sufficient to establish and maintain CML. In contrast, in Ph-positive B-ALL, additional mutations are frequently observed[8]. Various mouse models that express Bcr-Abl in hematopoietic stem cells or progenitor cells were developed and recapitulate many features of human CML and B-ALL[9,10]. Only a few studies have compared the *in vivo* leukemogenic activity of p190 and p210 directly. Under specific experimental conditions, the expression of p190 lead to a disease with a shorter latency and more B-ALL, whereas p210 mice developed CML-like leukemias[11,9,12,13]. This may argue that the specific intrinsic differences in the p190 and p210 proteins contribute to the two different disease pathologies, in addition to the described different cell-of-origin of the observed p210 and p190-driven leukemias[12]. Differences in activity and signaling between p210 and p190 have long been hypothesized but never studied in a comprehensive and quantitative manner. Early studies on selected signaling molecules indicated that qualitatively the same pathways are activated by p210 and p190[14], whereas kinase assays tended towards a mildly higher kinase activity for p190[11,15,16]. The p210 interaction network has been mapped by affinity purification mass spectrometry experiments with p210 interactors as baits using non-quantitative proteomics[17,18]. To date, very little is known regarding specific protein interaction partners and substrates of p190, and most importantly, the two Bcr-Abl isoforms have not been compared directly in a uniform cellular background.

Being aware of the large amount, but heterogeneous data regarding Bcr-Abl interacting proteins and activated downstream pathways, we performed a first

comparative, quantitative and systematic proteomics study to chart the common and differential interactome and tyrosine phosphoproteome of p210 and p190 Bcr-Abl. We show that the differences in interactome and phosphoproteome of p210 and p190 are surprisingly large despite similar kinase activation. Our study provides the first consolidated view on oncogene-intrinsic signaling differences of p210 and p190 in a defined cellular background.

Materials and Methods

Interactome sample preparation

The optimized final protocol used 80-100 mg total cell lysate per cell line, corresponding to approx. 7-10*10^8 BaF3 cells. Cell lysis and purification was performed in TAP buffer (50 mM TRIS pH 7.5, 100 mM NaCl, 5% glycerol, 0.2% (w/v) NP-40 Alternative) containing protease and phosphatase inhibitors [19]. Normal mouse IgG antibody (Thermo Scientific, catalog no. 10400C) and the monoclonal Abl antibody (clone 24-21)[20] were covalently coupled to NHS-activated sepharose (GE Healthcare, catalogue no. 17-0906-01). The lysates were pre-cleared for 1 h at 4°C with the IgG-NHS resin and the supernatant then transferred to the Abl-NHS resin for another 3 h at 4°C. Elution fractions containing Bcr-Abl were pooled prior to mixing of the three individual immunoprecipitates of BaF3 parental, p210 and p185 with equal volumes and subsequently lyophilized.

Phosphoproteome sample preparation

Cell lysis was accomplished in Urea buffer (8 M Urea, 50 mM Hepes, pH 7.6) using 2 mL buffer for $1*10^8$ cells. 10 mg of total cell lysate of each sample (light, medium and heavy labeled) were mixed to have a final amount of 30 mg SILAC sample for peptide preparation. Phosphotyrosine peptides were enriched using a mixture of two phosphotyrosine antibodies: The pY1000 antibody that is part of the PTMScan® Phospho-Tyrosine Rabbit mAb (P-Tyr-1000) Kit (Cell Signaling Technologies, catalogue number 8803), in addition to 50 µL NHS-coupled 4G10 antibody. For the pY eluates, a second step of phosphopeptide enrichment was performed on TiO_2 tips as described[21] prior MS analysis.

Data Analysis and MS raw data

A detailed description of the mass spectrometry data analysis to identify differential hits is given in Supplementary Information. Detailed lists of all interactors and phosphosites are provided in Supplementary Tables S4-S8 and an annotated Excel file with complete data. In addition, the mass spectrometry proteomics data have been deposited to the ProteomeXchange Consortium via the PRIDE partner repository with the dataset identifier PXD005149[22].

A detailed description of the methods used in this study is given in the Supplementary Methods.

Results

Bcr-Abl interactome analysis

To identify and quantify the protein interaction network of p210 and p190 Bcr-Abl, we used a quantitative proteomics workflow based on SILAC (stable isotope labeling with amino acids in cell culture; Fig. 1b). Murine BaF3 cells that express Abl endogenously were retrovirally transduced with the human Bcr-Abl p210 and p190 cDNAs[23] and purification of Bcr-Abl complexes was achieved by immunoprecipitation (IP) experiments using an immobilized anti-Abl antibody with 80-100 mg of total protein lysate in biological duplicates. Parental (untransduced) BaF3 cells were used as a control to distinguish (endogenous) Abl from Bcr-Abl interactors (Fig. 1b, Supplementary Table S1). We achieved the quantification of >1800 proteins and a strong enrichment of Bcr-Abl p210 and p190 complexes over the parental control (Fig. 2a, Supplementary Fig. S1a,b). Furthermore, we identified most of the previously suggested p210 core interactors[17], which we found to be enriched with Bcr-Abl compared to the parental control (Supplementary Fig. S1a, b).

To subsequently identify common Bcr-Abl interactors and proteins that preferentially or exclusively interact with either p210 or p190, we first identified proteins that are enriched in either p210 or p190 Bcr-Abl samples compared to the parental control (Fig. 2b). This strategy removed Abl interacting and contaminating proteins from further analysis. To compensate for the differential expression levels in the three different cell lines, we normalized the protein ratios for the input amounts, where ~4000 proteins of the expressed total proteome could be quantified (Fig. 2b). The resulting 147 proteins included 56 proteins that were common to both Bcr-Abl isoforms (defined as common Bcr-Abl interactors;

Supplementary Table S4), 30 proteins that were only found in the p210 samples and 59 proteins in the p190 samples (Fig. 2b). The excellent sequence coverage from the Bcr-Abl region common to p210 and p190 allowed a precise quantification of and subsequent correction for the Bcr-Abl bait amount in the large-scale IP samples (Supplementary Fig. S1c, d). For the comparison of the p210 and p190 interactors, this correction step is essential, because higher amounts of Bcr-Abl bait protein in one of the samples would lead to an overestimation of the amount of interactor. In both biological replicates p210 was ~1.4-fold enriched over p190 based on the mass spectrometry quantification (Fig. 2b, Supplementary Fig. S1c, d). After these normalization steps, we concentrated on those proteins that were at least 2-fold enriched, with 13 proteins for p210 and 34 proteins for p190 (Fig. 2c, Supplementary Table S5).

Common Bcr-Abl interactors

Among the 56 common Bcr-Abl interactors (Fig. 3, Supplementary Table S4), network analysis using the STRING database (http://string-db.org/) showed previously annotated experimentally determined interactions between the majority of these proteins. Only 15 molecules remain without previously mapped interactions (Supplementary Fig. S2a). Two major clusters were identified with one sub-network covering many cytosolic signaling components from tyrosine kinase and Ras-MAPK signaling pathways. These proteins include prototypic signaling adaptors (Grb2, Shc1, Dok1, Gab2), E3 ubiquitin ligases (Cbl, Cblb), phosphatases (Inppl1/Ship2 and Ptpn11/Shp2), kinases (Map4k1, Lrrk1),

GTPase effector proteins (including the Ras GEFs Sos1/2) and cytoskeleton remodeling proteins (e.g., the Abi1-Wasf2-Cyfip2 complex), which is also reflected in the KEGG pathway and GO term enrichment (Supplementary Fig. S2, Fig. 3). The three most significantly enriched domains using the SMART database were the SH2, SH3 and PH domains.

The very tightly interconnected second sub-network contained the tetrameric adaptor protein complex 2 (AP2), of which all four subunits were identified, with various associated proteins that play a key role in regulating clathrin-mediated endocytosis of receptor proteins and other membrane trafficking processes (Fig. 3). In addition to these two clusters, a small group of proteins with no previously experimentally mapped connections is included in the network of common Bcr-Abl interactors, such as the kinase co-chaperone Cdc37 and two members of the 14-3-3 proteins (Ywhag and Ywhah) (Fig. 3).

Notably, there is a large overlap of the mapped common Bcr-Abl interactors with the previously identified p210 Bcr-Abl interactors using non-quantitative proteomics by affinity purification mass spectrometry of known Bcr-Abl interacting adaptor proteins in either the human K562 cell line[17] or BaF3 cells[18]. Due to the use of SILAC, we achieve accurate quantitation and unbiased analyses.

Preferential and exclusive interactors of p210 and p190

The proteins that were differentially quantified between the two Bcr-Abl isoforms partly belong to the group of common Bcr-Abl interactors (preferential

interactors), whereas another fraction of proteins is exclusive to one of the Bcr-Abl isoforms and not part of the common Bcr-Abl interactome. With regard to p190 Bcr-Abl, 17 of the 34 identified proteins are also part of the common interactors including most of the AP2 complex members and the Nck2 (SH3/SH2 adaptor)-Rasa1 (Ras GAP)-Lyn (Src family tyrosine kinase) complex. The remaining 17 proteins are only found in p190 and include additional members of the endocytosis machinery, such as the clathrin light and heavy chains (Cltca/b/c) (Fig. 3, Supplementary Fig. S2 and Table S5).

Conversely, 3 of the 13 proteins that differentially bind to p210, are also part of the common Bcr-Abl interactors (Ubash3b/Sts1, Bcr and Shank3; Fig. 3, Supplementary Table S5). In contrast to p190, the differential proteins for p210 have no annotated experimental evidence for interaction with each other. Remarkably, the non-canonical tyrosine phosphatase Ubash3b/Sts1 shows a mean 6.5-fold enriched interaction with p210 Bcr-Abl (Fig. 2c).

Interactome target validation

Validation of the interactome data was conducted by immunoblot analysis of the SILAC samples used for the MS analysis as an independent analytical method. Furthermore, anti-Abl immunoprecipitations were conducted for a set of human p210 and p190 expressing cell lines that were derived from CML and B-ALL patients (Supplementary Table S3, Supplementary Figure S3). In addition, an independent set of BaF3 p210 and p190 cells was created and used as a further control.

We first focused on the tyrosine phosphatase Sts1 that was found as a common Bcr-Abl interactor and greatly enriched with p210 Bcr-Abl. The enrichment was confirmed in the immunoblot analysis of the SILAC samples (Fig. 2d) and the independent BaF3 set (Supplementary Fig. S3). For the human cell lines a less pronounced preference of Sts1 for p210 was observed (Supplementary Fig. S3). The interpretation of such experiments is severely challenged by the different Bcr-Abl and interactor expression levels in the human cell lines (Supplementary Fig. S3c), as well as the different cellular proteome background of the cells.

Validation of proteins that were enriched with p190 included Ap2a1/2, which is a subunit of the tetrameric AP2 complex, and the protein tyrosine kinase Lyn. Immunoblot analysis of the SILAC samples confirmed the findings by mass spectrometry (Fig. 2d). The validation of Lyn in the human cell lines was complicated by limited antibody sensitivity and differential antibody binding to human and mouse Lyn, but with a possible trend towards p190 (Supplementary Fig. S3). Nonetheless, this data is nicely in line with several Lyn tyrosine sites that are stronger phosphorylated in p190 cells.

Among the common interactors of p210 and p190, we validated the Inppl1/Ship2 interaction. Although the Ship2 antibody surprisingly did not recognize the mouse form of the protein, the human cells showed uniform interactions of Ship2 with p210 or p190 (Supplementary Fig. S3).

In conclusion, we found and validated intriguingly strong differences in the protein interaction network of p210 and p190. Interestingly, our dataset shows a number of proteins preferentially interacting with p190, even though the longer

isoform p210 contains the additional DH-PH domains. Our data thus suggests that the DH-PH domain does not act as a protein-interaction scaffold. Alternatively, a different degree of kinase activation could result in rewiring of the cellular signaling network and thus change Bcr-Abl interaction partners.

Analysis of phosphorylation sites and activity of p210 and p190 Bcr-Abl

To test our hypothesis of possible quantitative differences in p210 and p190 activation, we studied the kinase activation state of Bcr-Abl by mapping phosphorylation sites by mass spectrometry, immunoblotting for major activating phosphorylation sites, and *in vitro* kinase activity assays.

We could quantify 17 tyrosine phosphorylation sites of Bcr-Abl by mass spectrometry (Fig. 4a). As expected, the five tyrosine phosphorylation sites (Y554, Y644, Y844, Y852 and Y910) that are unique to the p210 sequence were found strongly enriched in the p210 sample. In contrast, Y177 was phosphorylated to almost identical levels in p210 and p190, in line with our interactome data showing equal amounts of Grb2, which binds Y177 via its SH2 domain (Fig. 4a). For the remaining Bcr-Abl phosphorylation sites, including Y412 in the activation loop and Y245, both commonly used Bcr-Abl activation markers[24], insignificant differences were observed (Fig. 4a). In parallel, we monitored the phosphorylation state of Y412 and Y245 by immunoblotting using the total cell lysates of the SILAC samples and the human cell lines. Whereas the BaF3 cells show a slight increase of pY245 in the p210 cells, there is no major difference for pY412 between the isoforms (Fig. 4b,c). The human cell

lines, albeit quite heterogeneous, revealed a higher tendency of both phosphorylation sites towards p210 (Fig. 4b,c). Similar results were obtained when equal amounts of Bcr-Abl after immunoprecipitation were loaded to facilitate normalization (Supplementary Fig. S4).

We next compared the Bcr-Abl *in vitro* kinase activity after anti-Abl immunoprecipitation from BaF3 and our panel of eight human cell lines. We observed only minor differences without a consistent trend towards higher *in vitro* kinase activity of one of the two Bcr-Abl isoforms (Fig. 4d). We additionally probed global p210 and p190 kinase activity using the PamChip PTK assay (PamGene). We observed only minor differences between the samples with only 7 of the 142 peptides phosphorylated stronger by the p210 lysate (Supplementary Fig. S5) in contrast to a previous study in which we compared Nup214-Abl and p210 activity in BaF3 cells[25].

Collectively, our data suggest that p210 and p190 do not differ significantly in kinase autophosphorylation or *in vitro* kinase activity. These results argue against quantitative differences in kinase activation may account for the observed differences in the p210 vs. p190 interactome and phosphoproteome.

Bcr-Abl phosphoproteome analysis

In addition to the phosphotyrosine sites of Bcr-Abl, we mapped the cellular tyrosine phosphoproteome and quantified 817 phosphotyrosine sites in 573 protein groups (Fig. 5a, Supplementary Fig. S6). Unsupervised hierarchical clustering of the quantified phosphopeptides revealed six clusters with cluster 1

288 comprising all the sites that remained unchanged among the three cell lines (Fig.
289 5a). Clusters 2, 3 and 4 depict the phosphopeptides that are up-regulated in the
290 Bcr-Abl cell lines compared to the parental cell line. Here in particular, clusters 2
291 and 3 (with 302 phosphopeptides corresponding to 37% of all quantified pY
292 peptides) stood out due to the high intensity of phosphorylation as compared to
293 the BaF3 parental cells, thus representing the Bcr-Abl pY signature (Fig. 5a).
294 Among those peptides, 45 sites map to 27 of the Bcr-Abl interacting proteins
295 identified in the interactome study, which makes it the cluster with the largest
296 accumulation of Bcr-Abl interactors (Supplementary Fig. S7). In-depth analysis of
297 the phosphosites within this cluster revealed many known and amply
298 characterized substrates of Bcr-Abl such as Abi1, Cbl, Gab2, Pik3r1, Pxn
299 (paxillin) and Stat5[26] that is also reflected in the GO term enrichment analysis of
300 these proteins containing CML and other tyrosine kinase signaling pathways
301 (Supplementary Fig. S7). In addition, phosphomotif analysis showed enrichment
302 of the Abl phosphorylation site consensus in cluster 2 and 3 (67 out of 273
303 unique peptides) with a proline in position +3 following the phosphorylated
304 tyrosine (Supplementary Fig. S7). Altogether, our dataset indicated that the
305 mapped tyrosine phosphoproteome is dominated by Bcr-Abl kinase signaling
306 and included many known substrates and phosphorylated interactors (Fig. 3).
307

308 **Differential phosphorylation sites of p210 and p190**

309 The analysis of differential p210 and p190 phosphorylation events resulted in
310 106 pY sites in 78 proteins to be more highly phosphorylated in p190, 110 pY

311 sites in 92 proteins to be more highly phosphorylated in p210 (Fig. 5b and
312 Supplementary Table S6 and S7).
313 Among the sites up-regulated in p210, 6 phosphorylation sites of the
314 transcription factor Stat5a and Stat5b were mapped, including the main site
315 responsible for Stat5a activation (Y694 in Stat5a, Fig. 6, Supplementary Table
316 S7)[27]. In addition, the activation loops of the tyrosine kinase Fes (Y713) and the
317 Ser/Thr-kinases Erk1 (Y205) and Erk2 (Y185) and sites of the Src family kinases
318 Fyn (Y185) and Lck (Y192), were found to be more highly phosphorylated (Fig.
319 6). This indicated a higher activation of these kinases in the p210 expressing
320 cells. The high number of kinases that are phosphorylated in the p210 sample is
321 also reflected in the GO term and KEGG pathway enrichment analysis
322 (Supplementary Fig. S7).
323 Among the 106 pY sites up-regulated in p190, 6 phosphosites of the Src family
324 tyrosine kinase Lyn (two of which shared with Blk), including its activation loop
325 (Y397) were found to be more strongly phosphorylated than in p210 (Fig. 6). This
326 is nicely in line with the stronger interaction of Lyn with p190 than p210 (Fig. 2c).
327 In addition the non-receptor tyrosine phosphatases Shp2 (Ptpn11) and Flk1
328 (Ptpn18) showed higher phosphorylation in p190 cells, which may indicate a
329 stronger activation of these enzymes in p190 cells. Furthermore, we found the
330 adapter proteins Dok1 and Pag1 to be more highly phosphorylated in p190, and
331 they, together with Ptpn11 and Ptpn18 were shown to play a central role in the
332 negative feedback regulation of Src family kinases (Fig. 6)[28].

Noteworthy, among the 552 pY sites that remain unchanged between the two Bcr-Abl isoforms, we found many central signaling molecules mediating pY signaling (Supplementary Table S8). These included adaptor proteins (CrkL, Shc1, Gab2, Nck1/2, Abi1/2, Dok1/2/3, Sh2d3/5, Skap2, several 14-3-3 isoforms), E3 ubiquitin ligases (Cbl, Cblb), lipid and protein phosphatases (Inppl1/5d, Ptpn6, Ptprc, Ptprj), several PI3-kinase subunits and the transcription factor Stat6. In addition, a large number of activating pY sites on cytoplasmic tyrosine kinases (Btk, Tec, Jak2, Csk, Tnk2, Syk) as well as serine/threonine kinases (Cdk1/17, Mapk14/11/12 = p38α/β/γ, Sgk233, Map4k1, Pkcδ) were found (Fig. 6 and Supplementary Table S8). This shows the large deregulation of cellular signaling by Bcr-Abl and its link to core proliferative and anti-apoptotic pathways that sustain leukemogenesis. Collectively, our analysis identified many differentially regulated phosphosites with annotated functional importance along with a large number of functionally uncharacterized sites in important signaling proteins.

Phosphoproteome site validation

Validation of the phosphoproteomic dataset was conducted by immunoblot analysis of the SILAC samples in addition to the set of human p210 and p190 Bcr-Abl expressing cell lines (Supplementary Table S3). Among the 6 up-regulated Stat5a/b phosphorylation sites in p210, we concentrated on Y694/Y695 in Stat5a/b, since it is the major activating site. We could confirm the MS results in BaF3 and human CML cell lines (Fig. 5c, d). In line with the

analysis of the total BaF3 Stat5 protein amount by MS, we also observed elevated Stat5 expression levels in p210 expressing cells. Nonetheless, pStat5 levels were increased also after correction for the elevated total protein levels showing increased Stat5 phosphorylation stoichiometry in p210 cells (Fig. 5c, d). Another member of the Stat transcription factors, Stat3, also showed elevated phosphorylation on the main activating site (Y704) in p210 in line with the MS results (Supplementary Fig. S8). In contrast, we found Stat6 to be equally phosphorylated on its main activating site (Y641; Fig. 6)

Src family kinases were found phosphorylated in both Bcr-Abl cell lines with Lyn being activated in p190 cells, and Fyn and Lck phosphorylation being higher in p210 cells. Due to the high sequence homology within this kinase family, antibodies for the activation loop of Src kinases cannot distinguish the different kinases of this family. Nonetheless, we attempted to monitor pSrc levels in our cell lines and found higher general pSrc levels in BaF3 p190 cells compared to the human cell lines, in which we observed a trend towards higher pSrc levels in the p210 Bcr-Abl cells (Supplementary Figure S8). A clear interpretation of this data is difficult, as the human cell lines have strongly different Src kinase expression patterns and levels. Therefore, reliable normalization of the pSrc signal is impossible. Interestingly, tyrosine kinase prediction based on the analysis of the PamChip PTK assay indicated overall stronger activation of Src kinases in p210 cells (Supplementary Fig S5). In contrast, we used an antibody that is specific for the C-terminal inhibitory phosphorylation site of Lyn (Y507) because we found several proteins of the Src negative-feedback circuit

phosphorylated in p190. Immunoblot analysis showed higher levels of pY507 phosphorylation in Bcr-Abl expressing BaF3 cells as compared to the parental cells but did not appear to differ between the two isoforms (Supplementary Fig. S8). The same was found for the human cell lines, where high levels of Lyn pY507 correlate with a high expression level.

Kinase activity profiling on the PamChip STK assay (PamGene) revealed a much higher activity of Ser/Thr kinases in the lysate of p210 with more than 20% of the peptides being more phosphorylated as compared to the p190 lysate. The prediction of putative upstream kinases from these data suggested the involvement of Sgk2, Akt and Dclk2 (Supplementary Fig. S5).

In summary, we found strongly activated Stat5 in p210, Dok1 in p190, and Src kinase members appear to be differentially activated by p210 and p190. In line with the observations of an isoform-dependent interactome, also the phosphoproteome varies significantly with the Bcr-Abl isoform and suggests important differential signaling nodes with possible therapeutic implications (Fig. 7).

Discussion

We observed many differences in both the interactome and the phosphoproteome between the two Bcr-Abl isoforms (Fig. 3 and 6). Because p190 can be considered as an internal deletion mutant of p210, lacking 501 amino acids that encode for a DH-PH domain unit, significant gains in the p210 interactome were expected rather than the observed balanced number of

interactors, excluding a scaffolding function of the DH-PH domain. This observation raises questions regarding the molecular mechanism. Our initial hypothesis on a different degree of kinase activity deregulation could be excluded. Even in BaF3 cells, i.e. in the same proteomic 'background', differences in kinase activation were insignificant. In line with this, the human cell lines also showed no consistent differences of p210 and p190 Bcr-Abl kinase activation. It is also unlikely to assume that the different length of the Bcr portion of p190 and p210 may change substrate specificity because the substrate binding groove in the kinase domain primarily determines the kinase substrate specificity, which is identical in p210 and p190. A second attractive hypothesis includes a possible differential subcellular localization that is caused by the different overall structure and domain composition of the two isoforms. As a result, p210 would encounter another subset of the proteome than p190 and would consequently differentially activate signaling pathways due to different interacting proteins, including kinases and phosphatases, ultimately resulting in pronounced differences in the phosphoproteome. In line with this hypothesis, deletion of the F-actin binding domain in p210 and p190 was found to have different effects on the leukemogenicity of Bcr-Abl[29,30,31]. In addition, the presence of the largely uncharacterized PH domain in p210 may play an important role in differential subcellular localization. PH domains are classical phosphoinositide-binding domains and mediate targeting of PH-domain containing proteins to membranes. If the p210 PH domain is important for Bcr-Abl localization, however, needs to be clarified by future studies. Similarly, we

found that the AP2 adaptor protein complex and associated proteins strongly and preferentially interact with p190 (Fig. 7). The tetrameric AP2 complex mediates the internalization of membrane receptors by regulating the assembly of clathrin-coated pits resulting in endocytosis. The functional consequences of the 'hijacking' of the AP2 complex on Bcr-Abl localization or receptor trafficking in p190 cells warrant in-depth future analysis. Among the strongest differential interactors of p210, we found the non-canonical tyrosine phosphatase Sts-1, which was described as a negative regulator of the Zap-70 tyrosine kinases in T-cell receptor signaling[32]. It is tempting to speculate that its strong interaction with p210 might be a mechanism to negatively regulate Bcr-Abl (Fig. 7).

Among the strongest up-regulated phosphorylation events in p210 was Stat5 on 6 tyrosine phosphorylation sites, including the major site that activates Stat5 dimerization, nuclear translocation and transcriptional activation (Fig. 7). Importantly, Stat5 is an essential Achilles heel in CML, as it is absolutely required for disease initiation, as well as disease maintenance and Stat5 upregulation mediates TKI resistance[33,34]. Interestingly, the strong activation of Stat5 by p210 but not p190 is mirrored by our previous data on the requirement of the upstream JAK2 kinase for initial lymphoid transformation by p190 (or v-Abl) but not myeloid transformation by p210[13]. These findings have important obvious implications for the ongoing studies of Jak2 TKIs in Ph-positive leukemias.

Another critical class of downstream signaling mediators of Bcr-Abl are the Src kinases. We found that the Src family kinase Lyn and its interactor Hcls1 (hematopoietic cell-specific Lyn substrate 1) show stronger interactions with

p190 than p210 and that Lyn further shows stronger phosphorylation in p190 cells at 6 sites, including the activation loop (Fig. 7). Lyn, along with Hck and Fgr, was shown to be required for B-lymphoid, but not myeloid transformation[35]. Lyn upregulation was shown to mediate imatinib resistance[36], and lymphoid, but not myeloid blast crisis CML cells are strongly dependent on Lyn expression and activity[37]. Similarly, the Fes tyrosine kinase that we found activated by p210 was previously shown to drive myeloid differentiation in K562 cells[38].

Collectively, these examples show that the mapped differential activation of tyrosine kinase and phosphatase pathways may indeed be tightly associated or causal to drive either myeloid or B-lymphoid transformation by p210 or p190. Finally, these kinases are readily druggable targets that may help patients to better cope with TKI resistance and offer more effective treatment options, particularly for Ph-positive B-ALL patients.

Acknowledgements

This work was supported by the ISREC Foundation (S.R., S.G. and O.H.), Swiss National Science Foundation (grant 31003A_140913; S.R. and O.H.), National Center of Competence in Research (NCCR) in Chemical Biology (O.H.). We thank B. Correia for his critical input on the manuscript, EPFL Protein Expression Core Facility for help with antibody production and all members of the Hantschel lab for continuous support and discussions. OH wishes to dedicate this paper to the memory of Dr. John Goldman.

Competing Interests

The authors declare that they have no financial and non-financial competing interests.

References

1. O'Hare T, Zabriskie MS, Eiring AM, Deininger MW. Pushing the limits of targeted therapy in chronic myeloid leukaemia. *Nature Reviews Cancer* 2012; **12:** 513-526.

2. Wong S, Witte ON. The BCR-ABL Story: Bench to Bedside and Back. *Annu Rev Immunol* 2004; **22:** 247-306.

3. Deininger MW, Goldman JM, Melo JV. The molecular biology of chronic myeloid leukemia. *Blood* 2000; **96:** 3343-3356.

4. Hantschel O. Structure, regulation, signaling, and targeting of abl kinases in cancer. *Genes Cancer* 2012; **3:** 436-446.

5. Gambacorti-Passerini C, Antolini L, Mahon F-X, Guilhot F, Deininger M, Fava C*, et al.* Multicenter independent assessment of outcomes in chronic myeloid leukemia patients treated with imatinib. *J Natl Cancer Inst* 2011; **103:** 553-561.

6. Fielding AK. How I treat Philadelphia chromosome positive acute lymphoblastic leukaemia. *Blood* 2010; **116:** 3409-3417.

7. Rousselot P, Coude MM, Gokbuget N, Gambacorti Passerini C, Hayette S, Cayuela JM*, et al.* Dasatinib and low-intensity chemotherapy in elderly patients with Philadelphia chromosome-positive ALL. *Blood* 2016; **128:** 774-782.

8. Mullighan CG, Downing JR. Genome-wide profiling of genetic alterations in acute lymphoblastic leukemia: recent insights and future directions. *Leukemia* 2009; **23:** 1209-1218.

9. Wong S, Witte ON. Modeling Philadelphia chromosome positive leukemias. *Oncogene* 2001; **20:** 5644-5659.

10. Van Etten RA. Studying the pathogenesis of BCR-ABL+ leukemia in mice. *Oncogene* 2002; **21:** 8643-8651.

11. Li S, Ilaria RL, Jr., Million RP, Daley GQ, Van Etten RA. The P190, P210, and P230 forms of the BCR/ABL oncogene induce a similar chronic myeloid

leukemia-like syndrome in mice but have different lymphoid leukemogenic activity. *J Exp Med* 1999; **189:** 1399-1412.

12. Kovacic B, Hoelbl A, Litos G, Alacakaptan M, Schuster C, Fischhuber KM*, et al.* Diverging fates of cells of origin in acute and chronic leukaemia. *EMBO Mol Med* 2012.

13. Hantschel O, Warsch W, Eckelhart E, Kaupe I, Grebien F, Wagner K-U*, et al.* BCR-ABL uncouples canonical JAK2-STAT5 signaling in chronic myeloid leukemia. *Nat Chem Biol* 2012; **8:** 285-293.

14. Okuda K, Golub TR, Gilliland DG, Griffin JD. p210BCR/ABL, p190BCR/ABL, and TEL/ABL activate similar signal transduction pathways in hematopoietic cell lines. *Oncogene* 1996; **13:** 1147-1152.

15. Lugo TG, Pendergast AM, Muller AJ, Witte ON. Tyrosine kinase activity and transformation potency of bcr-abl oncogene products. *Science* 1990; **247:** 1079-1082.

16. Ilaria RL, Jr., Van Etten RA. The SH2 domain of P210BCR/ABL is not required for the transformation of hematopoietic factor-dependent cells. *Blood* 1995; **86:** 3897-3904.

17. Brehme M, Hantschel O, Colinge J, Kaupe I, Planyavsky M, Kocher T*, et al.* Charting the molecular network of the drug target Bcr-Abl. *Proc Natl Acad Sci U S A* 2009; **106:** 7414-7419.

18. Titz B, Low T, Komisopoulou E, Chen SS, Rubbi L, Graeber TG. The proximal signaling network of the BCR-ABL1 oncogene shows a modular organization. *Oncogene* 2010; **29:** 5895-5910.

19. Burckstummer T, Bennett KL, Preradovic A, Schutze G, Hantschel O, Superti-Furga G*, et al.* An efficient tandem affinity purification procedure for interaction proteomics in mammalian cells. *Nat Methods* 2006; **3:** 1013-1019.

20. Schiff-Maker L, Burns MC, Konopka JB, Clark S, Witte ON, Rosenberg N. Monoclonal antibodies specific for v-abl- and c-abl-encoded molecules. *J Virol* 1986; **57:** 1182-1186.

21. Kettenbach AN, Gerber SA. Rapid and reproducible single-stage phosphopeptide enrichment of complex peptide mixtures: application to general and phosphotyrosine-specific phosphoproteomics experiments. *Anal Chem* 2011; **83:** 7635-7644.

22. Vizcaino JA, Csordas A, del-Toro N, Dianes JA, Griss J, Lavidas I*, et al.* 2016 update of the PRIDE database and its related tools. *Nucleic Acids Res* 2016; **44:** D447-456.

539 23. Warmuth M, Kim S, Gu XJ, Xia G, Adrian F. Ba/F3 cells and their use in
540 kinase drug discovery. *Curr Opin Oncol* 2007; **19:** 55-60.

541 24. Hantschel O, Superti-Furga G. Regulation of the c-Abl and Bcr-Abl
542 Tyrosine Kinases. *Nat Rev Mol Cell Biol* 2004; **5:** 33-44.

543 25. De Keersmaecker K, Versele M, Cools J, Superti-Furga G, Hantschel O.
544 Intrinsic differences between the catalytic properties of the oncogenic NUP214-
545 ABL1 and BCR-ABL1 fusion protein kinases. *Leukemia* 2008; **22:** 2208-2216.

546 26. Ren R. Mechanisms of BCR-ABL in the pathogenesis of chronic
547 myelogenous leukaemia. *Nat Rev Cancer* 2005; **5:** 172-183.

548 27. Shuai K, Horvath CM, Huang LH, Qureshi SA, Cowburn D, Darnell JE, Jr.
549 Interferon activation of the transcription factor Stat91 involves dimerization
550 through SH2-phosphotyrosyl peptide interactions. *Cell* 1994; **76:** 821-828.

551 28. Rubbi L, Titz B, Brown L, Galvan E, Komisopoulou E, Chen SS*, et al.*
552 Global phosphoproteomics reveals crosstalk between bcr-abl and negative
553 feedback mechanisms controlling SRC signaling. *Science Signaling* 2011; **4:**
554 ra18.

555 29. Heisterkamp N, Voncken JW, Senadheera D, Gonzalez-Gomez I,
556 Reichert A, Haataja L*, et al.* Reduced oncogenicity of p190 Bcr/Abl F-actin-
557 binding domain mutants. *Blood* 2000; **96:** 2226-2232.

558 30. Wertheim JA, Perera SA, Hammer DA, Ren R, Boettiger D, Pear WS.
559 Localization of BCR-ABL to F-actin regulates cell adhesion but does not
560 attenuate CML development. *Blood* 2003; **102:** 2220-2228.

561 31. Hantschel O, Wiesner S, Guttler T, Mackereth CD, Rix LL, Mikes Z*, et al.*
562 Structural basis for the cytoskeletal association of Bcr-Abl/c-Abl. *Mol Cell* 2005;
563 **19:** 461-473.

564 32. Mikhailik A, Ford B, Keller J, Chen Y, Nassar N, Carpino N. A
565 phosphatase activity of Sts-1 contributes to the suppression of TCR signaling.
566 *Mol Cell* 2007; **27:** 486-497.

567 33. Hoelbl A, Schuster C, Kovacic B, Zhu B, Wickre M, Hoelzl MA*, et al.* Stat5
568 is indispensable for the maintenance of bcr/abl-positive leukaemia. *EMBO Mol*
569 *Med* 2010; **2:** 98-110.

570 34. Warsch W, Kollmann K, Eckelhart E, Fajmann S, Cerny-Reiterer S, Holbl
571 A*, et al.* High STAT5 levels mediate imatinib resistance and indicate disease
572 progression in chronic myeloid leukemia. *Blood* 2011; **117:** 3409-3420.

573 35. Hu Y, Liu Y, Pelletier S, Buchdunger E, Warmuth M, Fabbro D*, et al.*
574 Requirement of Src kinases Lyn, Hck and Fgr for BCR-ABL1-induced B-

lymphoblastic leukemia but not chronic myeloid leukemia. *Nat Genet* 2004; **36:** 453-461.

36. Wu J, Meng F, Kong LY, Peng Z, Ying Y, Bornmann WG*, et al.* Association between imatinib-resistant BCR-ABL mutation-negative leukemia and persistent activation of LYN kinase. *J Natl Cancer Inst* 2008; **100:** 926-939.

37. Ptasznik A, Nakata Y, Kalota A, Emerson SG, Gewirtz AM. Short interfering RNA (siRNA) targeting the Lyn kinase induces apoptosis in primary, and drug-resistant, BCR-ABL1(+) leukemia cells. *Nat Med* 2004; **10:** 1187-1189.

38. Yu G, Smithgall TE, Glazer RI. K562 leukemia cells transfected with the human c-fes gene acquire the ability to undergo myeloid differentiation. *J Biol Chem* 1989; **264:** 10276-10281.

Figure legends

Figure 1. Bcr-Abl domain organization and workflow of the proteomics experiments.

(a) The Abl tyrosine kinase and the two isoforms of the fusion protein Bcr-Abl, p210 and p190, are shown with their sizes and domain arrangement. The p210 isoform is 501 amino acids longer than p190 as it contains the DH-PH tandem domains. Domain abbreviations: CC: coiled-coil, DH: Dbl-homology, PH: Pleckstrin-homolgy, SH3/SH2: Src-homology 3/2, FABD: F-actin binding domain. (b) SILAC labeling was employed to allow quantitative comparison of three BaF3 cell lines (Supplementary Table S1). BaF3 parental cells express Abl endogenously. BaF3 p210 and BaF3 p190 cells express human Bcr-Abl p210 and p190. An immuno-affinity purification strategy was used to enrich for Bcr-Abl complexes for the interactome analysis and sample mixing was performed just prior peptide preparation. For analysis of the tyrosine phosphoproteome cell lysates were mixed prior enrichment of the pY peptides using the pY1000 and 4G10 antibodies and an additional TiO_2 purification step. For both experiments, the analysis of the total proteome served for different normalization steps.

Figure 2. Analysis of the Bcr-Abl p210 and p190 interactome.

(a) Quality control anti-Abl immunoblot after immuno-affinity purification of the Bcr-Abl complexes for a representative experiment. For the lysate samples 50 µg of total protein was loaded and an equivalent volume was used for the unbound fraction. The ratio of the two Bcr-Abl isoforms p210:p190 was 1.4:1 in the eluate,

which was in accordance with the quantification by mass spectrometry (Supplementary Fig. S1). For the elution fraction, 0.7% of the total SILAC eluate was loaded and quantification of bands enabled the calculation of the IP efficiency/Bcr-Abl complex recovery of 29% of the input amount.

(b) Schematic representation of filtering criteria to select the differential Bcr-Abl interactors. Quantified proteins (1888 and 3767 proteins, respectively) were normalized to their input amounts (4066 and 3989 proteins quantified, respectively) and only those proteins with significant enrichment (according to Significance B) over the parental control were selected. This reduced number of proteins were further normalized for the Bcr-Abl IP amounts and finally selected if differentially enriched by at least 2-fold. A detailed description of the data analysis workflow is described in the Supplementary Methods.

(c) Scatter plot representation depicting the final list of 147 Bcr-Abl interactors (58 common, 59 p190 enriched, 30 p210 enriched; see panel (b)) with the respective log2 ratios in both experiments (Bcr-Abl (BA) IP1 and IP2) showing an overall good correlation (R=0,72). Those proteins considered differential are colored in red (p210) and blue (p190). Selected proteins are highlighted with bigger dot size and gene name labels.

(d) Validation of differential Bcr-Abl interactors by immunoblotting. Elution fractions of both replicates were analyzed corresponding to 0.7% of the total SILAC elution fraction. We chose to validate the interactome hits Ubash3B/Sts-1 (enriched in p210) and AP2a1/2 and Lyn (both enriched in p190). The quantified

signal after correction for the Bcr-Abl IP amounts is shown on the right side. Individual values are plotted together with the mean +/- SD.

Figure 3. Network of Bcr-Abl interacting proteins.

Common and differential interactors of Bcr-Abl p210 and p190 are shown and summarized in Supplementary Tables S4 and S5. Connections for the differential interactors are color-coded according to their log2 ratios (from 'light red' for a weak p210 enrichment, to 'dark red' for a strong p210 enrichment; 'light blue' for a weak p190 enrichment to 'dark blue' for a strong p190 enrichment). Boxes around the individual proteins are color-coded according to the function and a red frame indicates that the protein was also found phosphorylated in the phosphoproteome analysis. Note that certain proteins enriched with either of the two Bcr-Abl isoforms can also interact with the other isoform and thus have a connection to both proteins.

Figure 4. Bcr-Abl p210 and p190 phosphorylation sites and kinase activity.

(a) Several Bcr-Abl pY sites were quantified in our phosphoproteome dataset. The domain organization and location of the pY sites are shown and the sites are plotted together with their respective log2 ratio between p210/p190. Dots represent mean values +/- SD. 5 out of the 17 sites could only be quantified in one experiment. Residues are numbered according to the Bcr and Abl 1b protein numbering.

(b) Immunoblot analysis of the two autophosphorylation sites that are important for Abl catalytic activity: pY245 and pY412. Equal amounts of total cell lysates of the indicated BaF3 and human p210 and p190 expressing cell lines were loaded, immunoblotted with the indicated antibodies and quantified (see (c)). Note that only Bcr-Abl is phosphorylated on Y245 and Y412, while Abl is not or only very weakly phosphorylated on these sites.

(c) Quantified pY245 and pY412 immunoblot signals (from panel (b)) after normalization to the total Bcr-Abl protein in BaF3 (left two graphs) or human cell lines (right two graphs) from two replicates. Individual values are plotted together with the mean +/- SD.

(d) Bcr-Abl was immunoprecipitated from the indicated BaF3 and human p210 and p190 cell lines and a radioactive *in vitro* kinase activity was performed measuring phosphotransfer to an optimal Abl substrate peptide. Each kinase assay was run in triplicate for each immunoprecipitate and the resulting averaged activity value was normalized to the Bcr-Abl amount determined by immunoblot analysis. The bar graph shows the mean +/- SD from three biological replicates.

Figure 5. Bcr-Abl pY phosphoproteome.

(a) Heatmap representation of the 817 quantified phosphosites and their respective ratios in the comparison of the three samples: BaF3 parental, BaF3 p210 and BaF3 p190. The two biological replicates are plotted next to each other. The six clusters identified by unsupervised hierarchical clustering are highlighted.

(b) Scatter plot for the normalized log2 ratios between the p210 and p190 Bcr-Abl samples (without correction for the total protein levels) in both biological replicates (pY1 and pY2). Each dot is representative of a phosphopeptide. Those pY sites considered as differential are colored in red (p210) and blue (p190). Selected phosphorylation sites are labeled.

(c, d) Immunoblot validation of Stat5 pY694 using the BaF3 and human cell line panel. The quantified signals of two technical replicates were normalized to the total Stat5 protein and individual values are plotted together with the mean +/- SD.

Figure 6. Selected phosphorylation events of p210 and p190 Bcr-Abl.

A selection of differential and common Bcr-Abl phosphorylation sites that were found in the pY dataset is shown. The complete dataset is shown in Supplementary Table S6, S7 and S8. Boxes around the individual proteins are color-coded according to their function and a red frame indicates that a protein was also found in the interactome analysis.

Figure 7. Model of differential signaling networks of p210 and p190 Bcr-Abl.

The main differences in Bcr-Abl interactors and phosphorlyated proteins between p210 and p190 that we found, validated and discussed in this paper is summarized in this figure. As examples for common interactors/pY sites, the Ship2 phosphatase and the interaction of the Grb2/Sos complex with pY177 is shown. p210 shows stronger association with the Sts-1 phosphatase and higher

activation of the Stat5 transcription factor, as well as the Erk1/2 and Fyn/Lck kinases. p190 shows stronger association with the AP2 complex and clathrin, and higher activation of the Dok1 adaptor and the Lyn kinase.

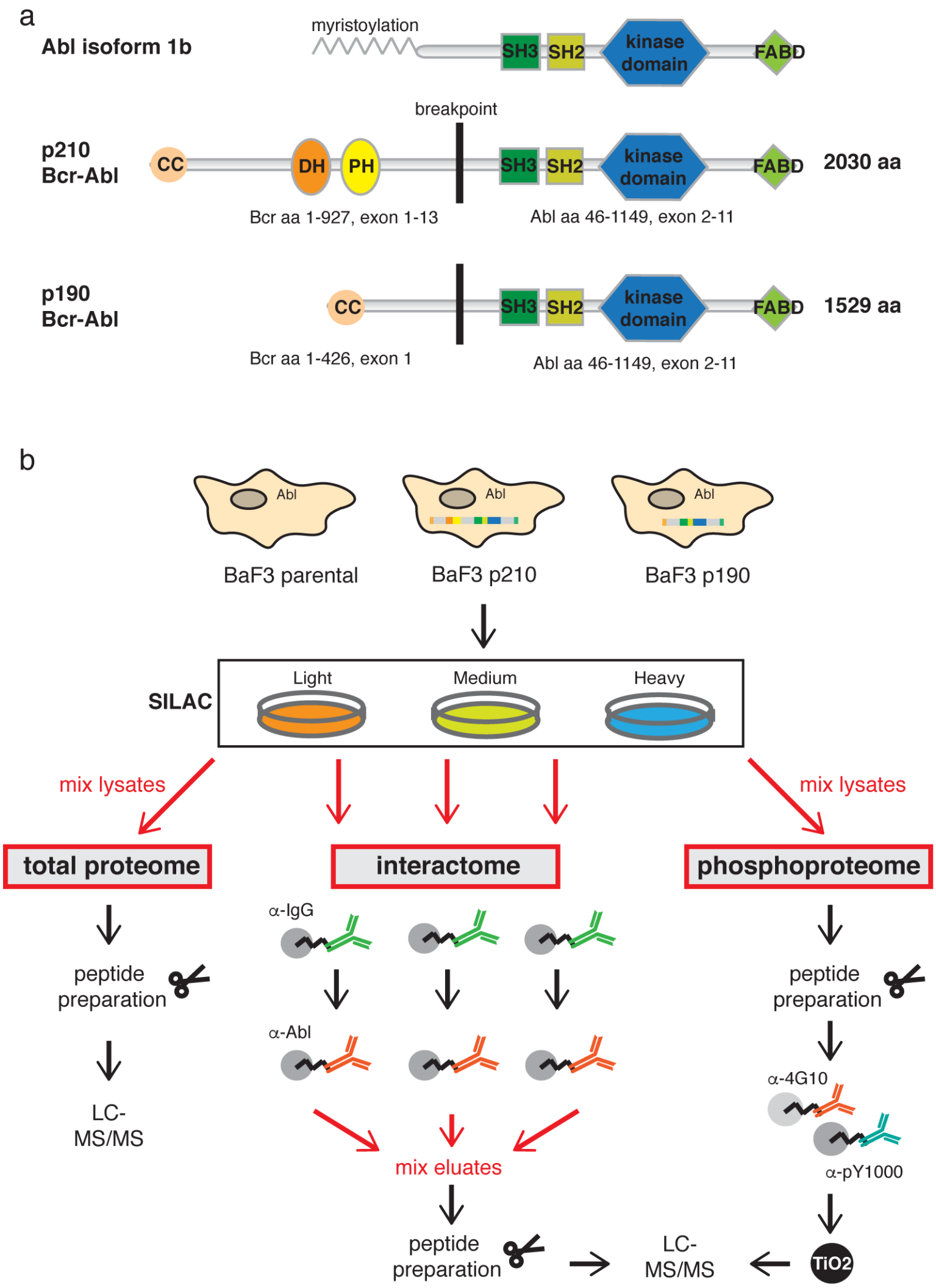
a
Abl isoform 1b
myristoylation
SH3
SH2
kinase domain
FABD
p210 Bcr-Abl
breakpoint
CC
DH
PH
2030 aa
Bcr aa 1-927, exon 1-13
Abl aa 46-1149, exon 2-11
p190 Bcr-Abl
1529 aa
Bcr aa 1-426, exon 1
b
Abl
BaF3 parental
BaF3 p210
BaF3 p190
SILAC
Light
Medium
Heavy
mix lysates
total proteome
interactome
phosphoproteome
peptide preparation
LC-MS/MS
α-IgG
α-Abl
mix eluates
α-4G10
α-pY1000
TiO2

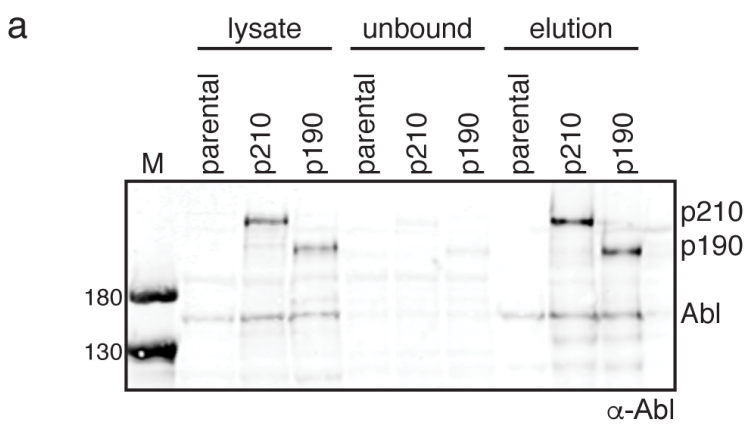
a
lysate
unbound
elution
parental
p210
p190
M
180
130
p210
p190
Abl
α-Abl

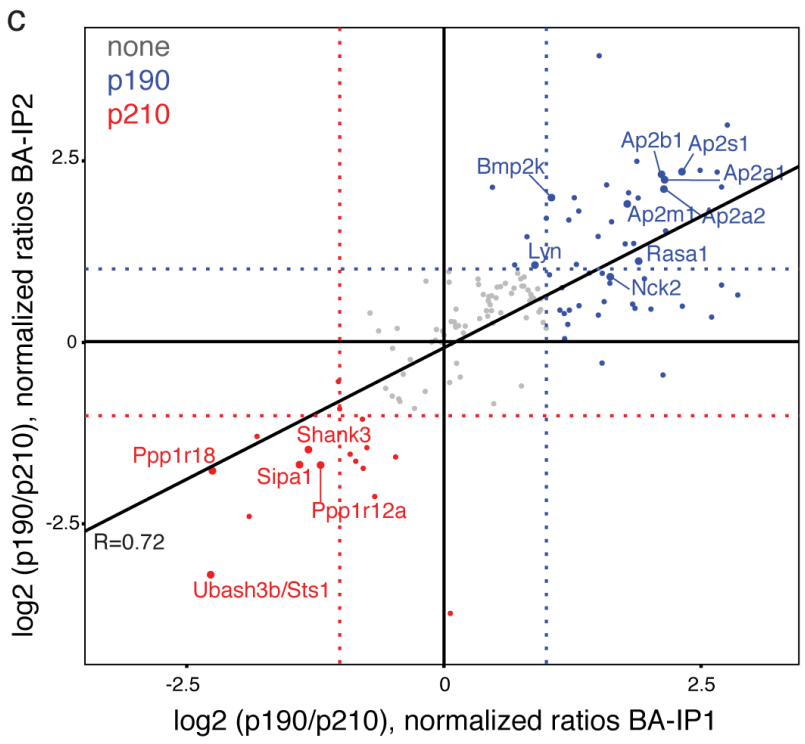
c
none
p190
p210
Ap2b1
Ap2s1
Ap2a1
Bmp2k
Ap2m1
Ap2a2
Lyn
Rasa1
Nck2
Shank3
Ppp1r18
Sipa1
Ppp1r12a
Ubash3b/Sts1
R=0.72
2.5
0
-2.5
log2 (p190/p210), normalized ratios BA-IP2
log2 (p190/p210), normalized ratios BA-IP1

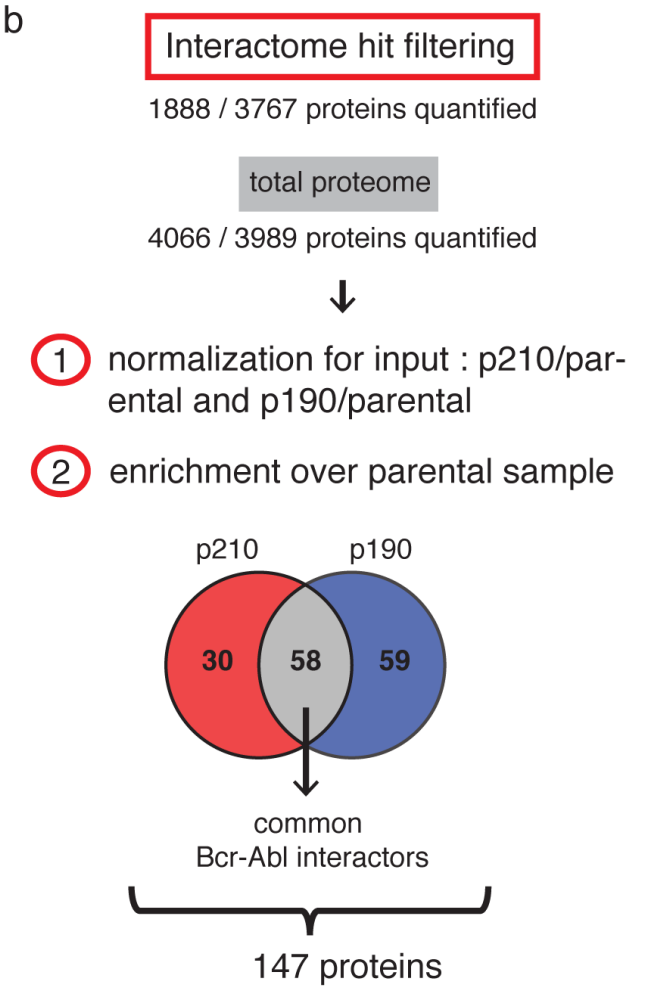
b
Interactome hit filtering
1888 / 3767 proteins quantified
total proteome
4066 / 3989 proteins quantified
1 normalization for input : p210/parental and p190/parental
2 enrichment over parental sample
p210
p190
30
58
59
common
Bcr-Abl interactors
147 proteins
3 normalization for input (p210/p190)
4 correction for Bcr-Abl IP level

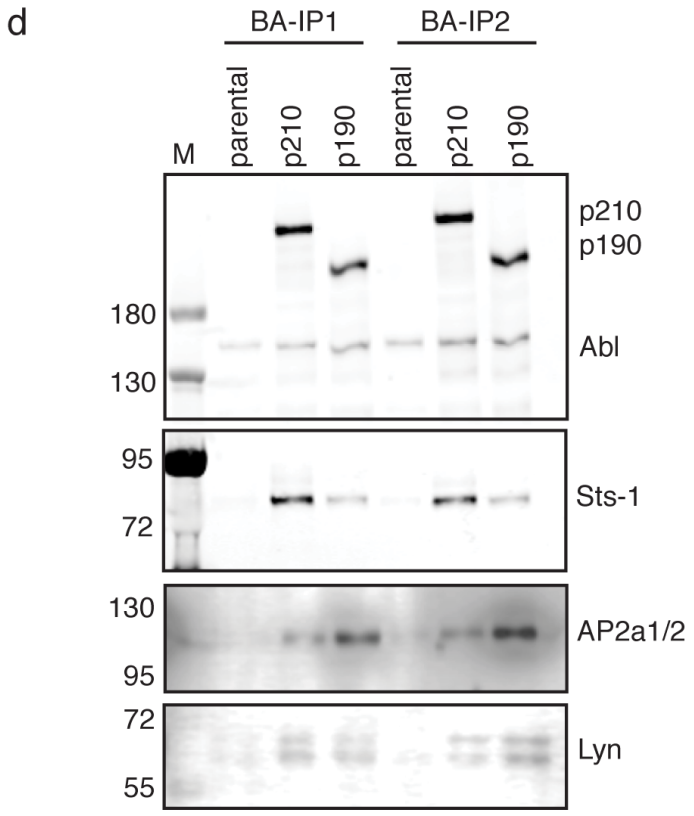
d
BA-IP1
BA-IP2
parental
p210
p190
M
180
130
p210
p190
Abl
95
72
Sts-1
130
95
AP2a1/2
72
55
Lyn

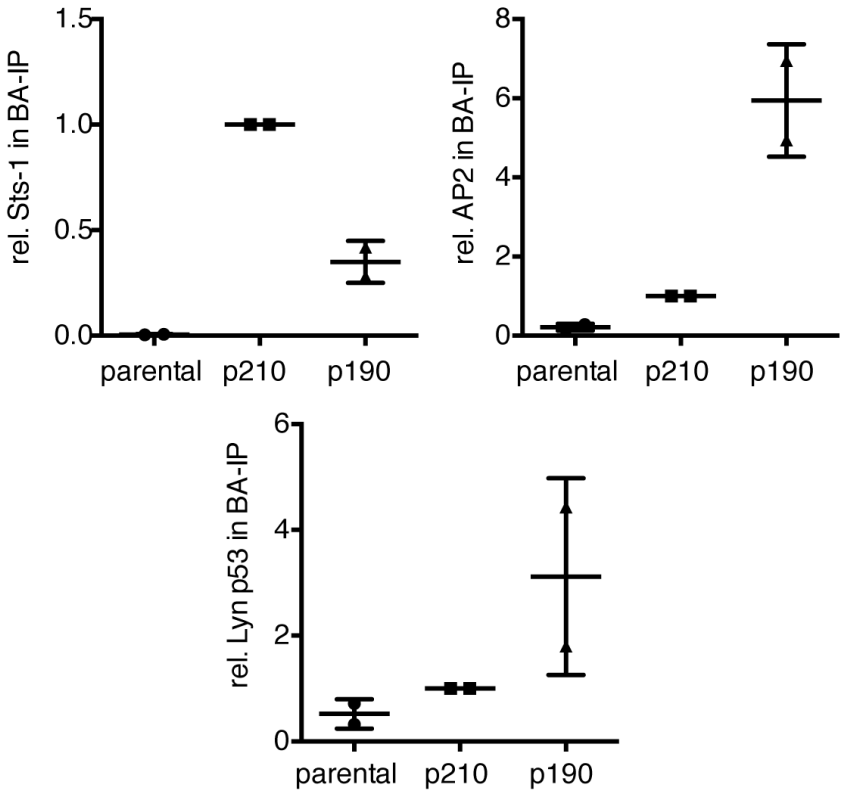
rel. Sts-1 in BA-IP
1.5
1.0
0.5
0.0
parental
p210
p190
rel. AP2 in BA-IP
8
6
4
2
0
parental
p210
p190
rel. Lyn p53 in BA-IP
6
4
2
0
parental
p210
p190

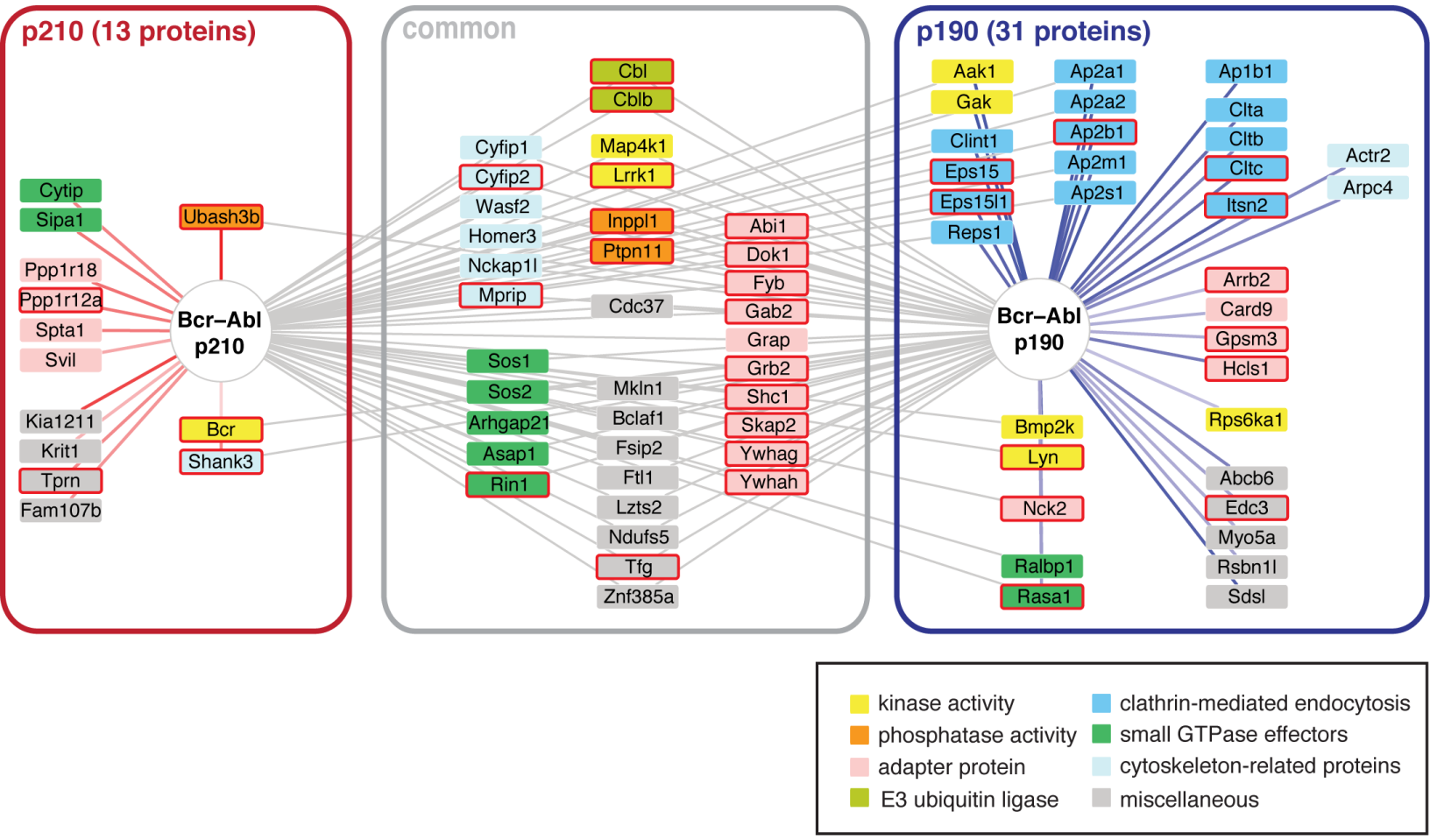
p210 (13 proteins)
Cytip
Sipa1
Ubash3b
Ppp1r18
Ppp1r12a
Spta1
Svil
Bcr–Abl p210
Kia1211
Krit1
Tprn
Fam107b
Bcr
Shank3
common
Cbl
Cblb
Cyfip1
Cyfip2
Wasf2
Homer3
Nckap1l
Mprip
Map4k1
Lrrk1
Inppl1
Ptpn11
Cdc37
Abi1
Dok1
Fyb
Gab2
Grap
Grb2
Shc1
Skap2
Ywhag
Ywhah
Sos1
Sos2
Arhgap21
Asap1
Rin1
Mkln1
Bclaf1
Fsip2
Ftl1
Lzts2
Ndufs5
Tfg
Znf385a
p190 (31 proteins)
Aak1
Gak
Clint1
Eps15
Eps15l1
Reps1
Ap2a1
Ap2a2
Ap2b1
Ap2m1
Ap2s1
Ap1b1
Clta
Cltb
Cltc
Itsn2
Actr2
Arpc4
Bcr–Abl p190
Arrb2
Card9
Gpsm3
Hcls1
Rps6ka1
Bmp2k
Lyn
Nck2
Ralbp1
Rasa1
Abcb6
Edc3
Myo5a
Rsbn1l
Sdsl
kinase activity
phosphatase activity
adapter protein
E3 ubiquitin ligase
clathrin-mediated endocytosis
small GTPase effectors
cytoskeleton-related proteins
miscellaneous

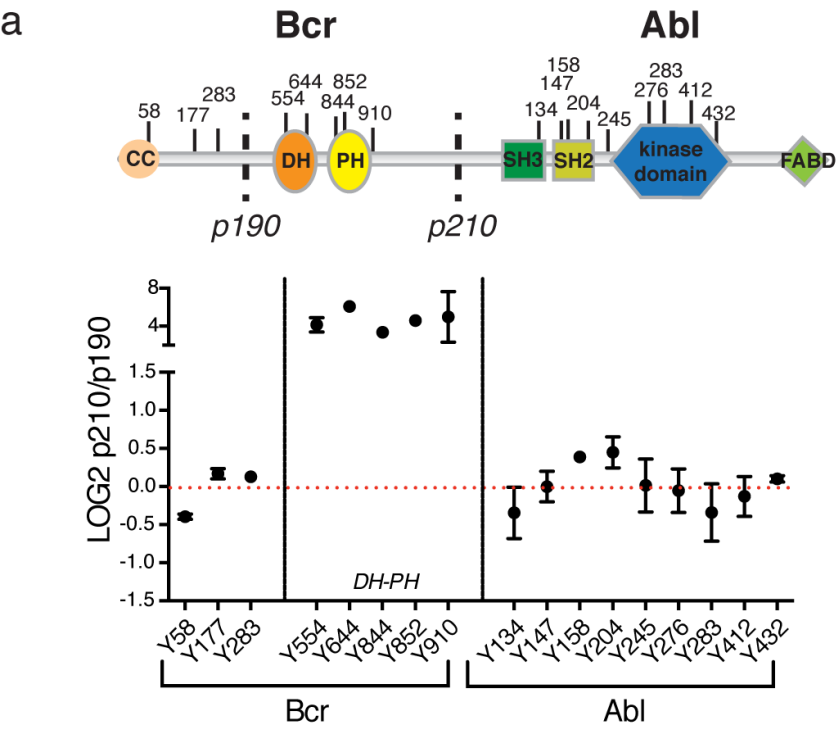
a
Bcr
Abl
58
177
283
554
644
852
844
910
134
147
158
204
245
276
283
412
432
CC
DH
PH
SH3
SH2
kinase domain
FABD
p190
p210
LOG2 p210/p190
DH-PH
Y58
Y177
Y283
Y554
Y644
Y844
Y852
Y910
Y134
Y147
Y158
Y204
Y245
Y276
Y283
Y412
Y432
Bcr
Abl

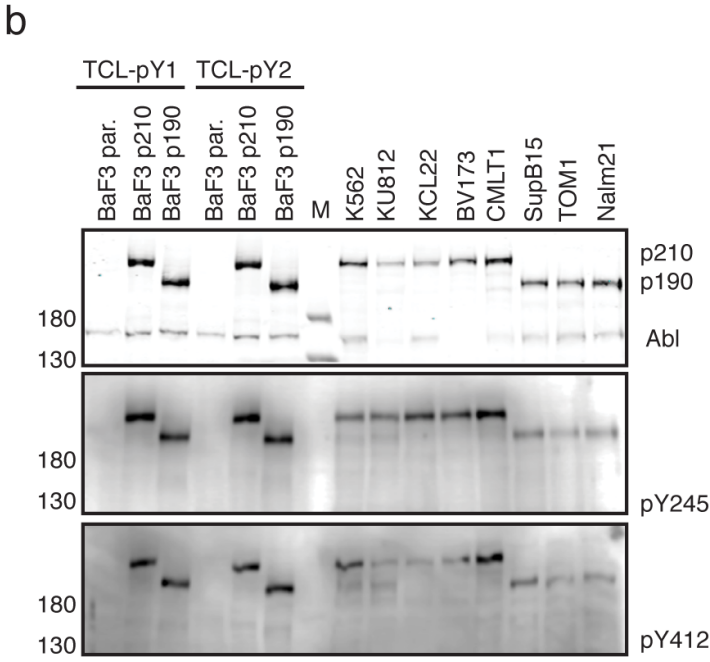
b
TCL-pY1
TCL-pY2
BaF3 par.
BaF3 p210
BaF3 p190
BaF3 par.
BaF3 p210
BaF3 p190
M
K562
KU812
KCL22
BV173
CMLT1
SupB15
TOM1
Nalm21
180
130
p210
p190
Abl
pY245
pY412

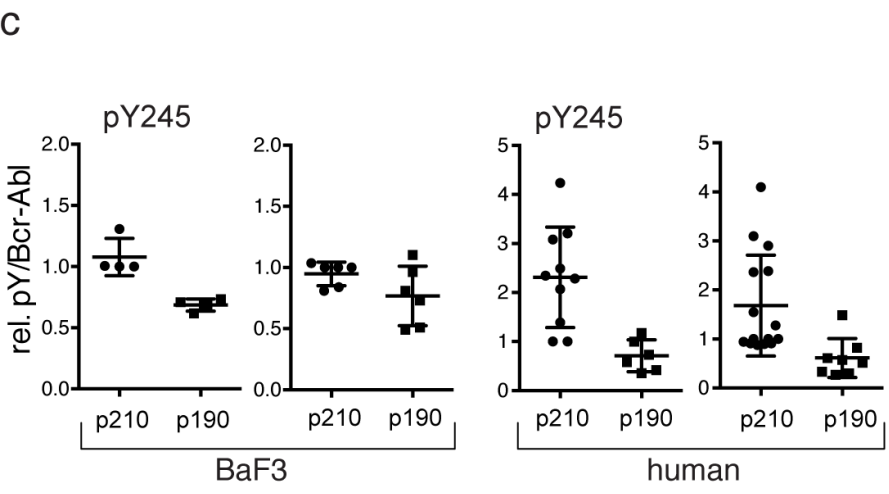
c
pY245
pY245
rel. pY/Bcr-Abl
p210
p190
BaF3
human

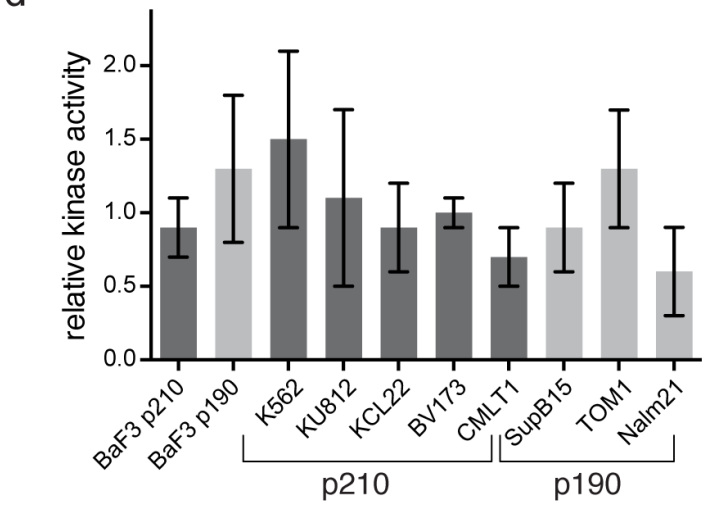
d
relative kinase activity
BaF3 p210
BaF3 p190
K562
KU812
KCL22
BV173
CMLT1
SupB15
TOM1
Nalm21
p210
p190

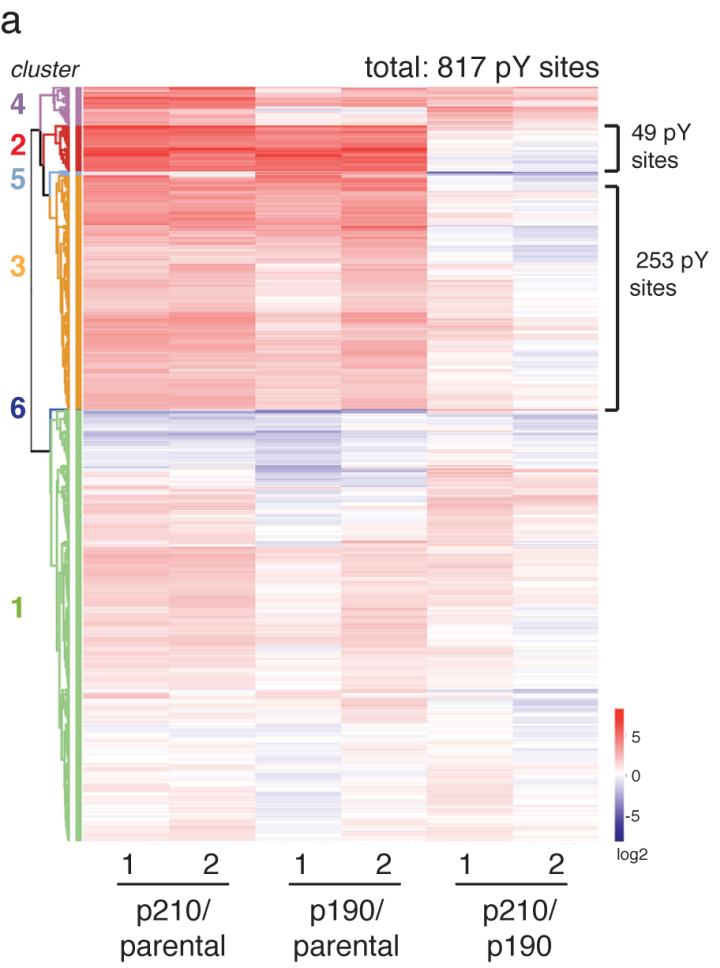
a
cluster
total: 817 pY sites
4
2
5
3
6
1
49 pY sites
253 pY sites
5
0
-5
log2
1 2 1 2 1 2
p210/ parental
p190/ parental
p210/ p190

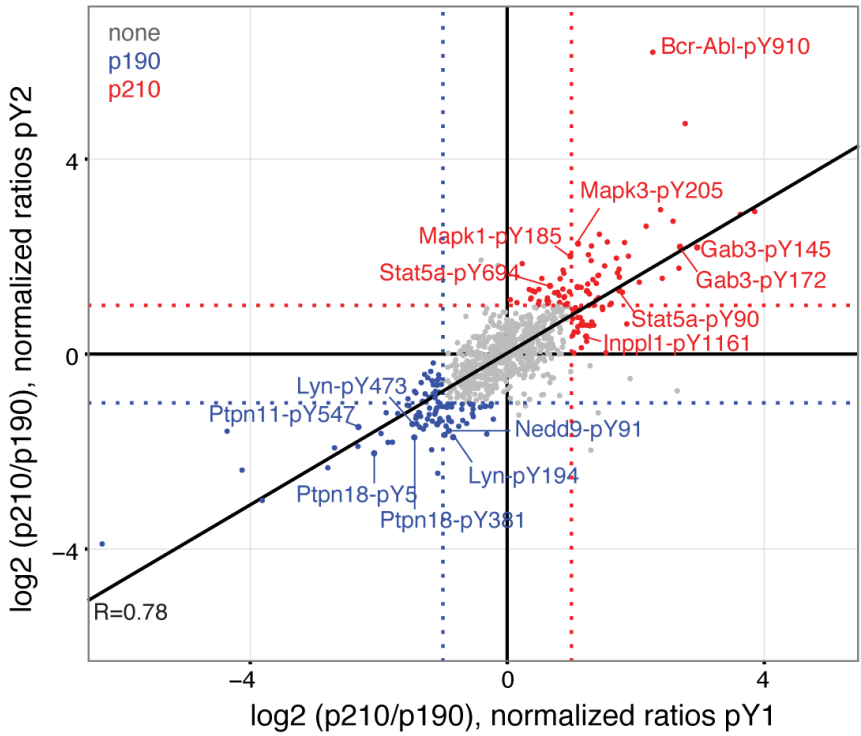
b
none
p190
p210
Bcr-Abl-pY910
Mapk3-pY205
Mapk1-pY185
Gab3-pY145
Stat5a-pY694
Gab3-pY172
Stat5a-pY90
Inppl1-pY1161
Lyn-pY473
Ptpn11-pY547
Nedd9-pY91
Lyn-pY194
Ptpn18-pY5
Ptpn18-pY381
R=0.78
log2 (p210/p190), normalized ratios pY2
log2 (p210/p190), normalized ratios pY1
4
0
−4
−4
0
4

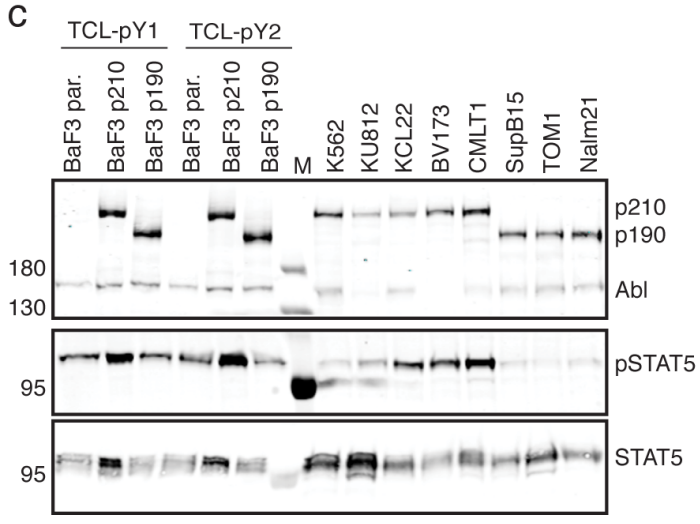
c
TCL-pY1
TCL-pY2
BaF3 par.
BaF3 p210
BaF3 p190
BaF3 par.
BaF3 p210
BaF3 p190
M
K562
KU812
KCL22
BV173
CMLT1
SupB15
TOM1
Nalm21
p210
p190
Abl
180
130
pSTAT5
95
STAT5
95

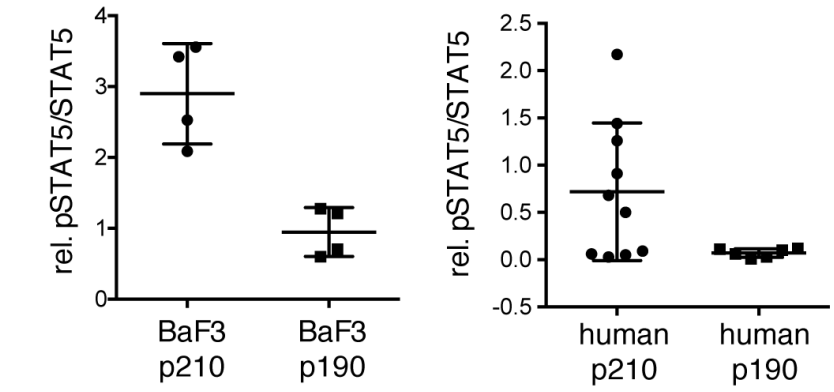
d
rel. pSTAT5/STAT5
4
3
2
1
0
BaF3 p210
BaF3 p190
rel. pSTAT5/STAT5
2.5
2.0
1.5
1.0
0.5
0.0
-0.5
human p210
human p190

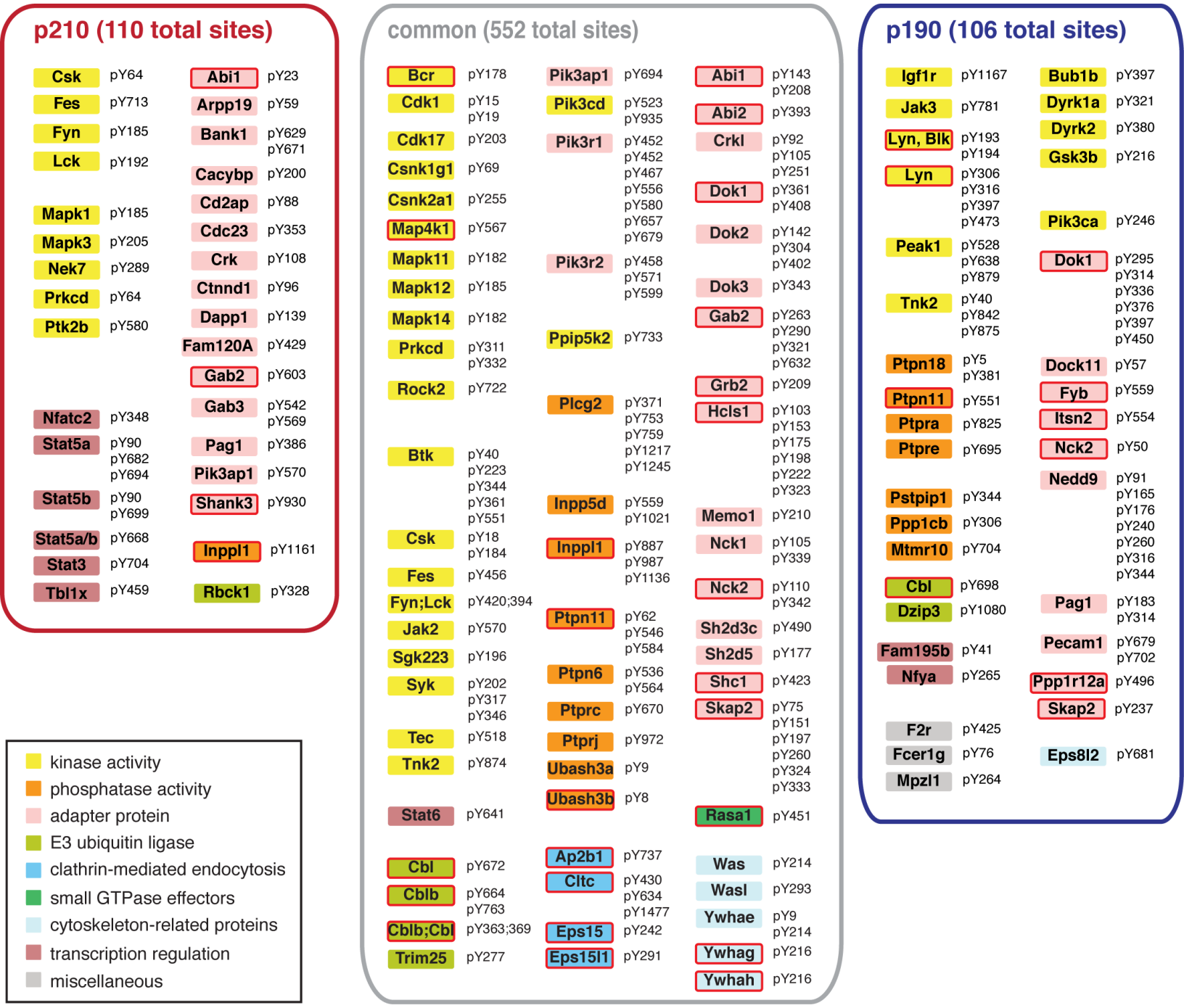
p210 (110 total sites)
Csk pY64
Fes pY713
Fyn pY185
Lck pY192
Mapk1 pY185
Mapk3 pY205
Nek7 pY289
Prkcd pY64
Ptk2b pY580
Nfatc2 pY348
Stat5a pY90 pY682 pY694
Stat5b pY90 pY699
Stat5a/b pY668
Stat3 pY704
Tbl1x pY459
Abi1 pY23
Arpp19 pY59
Bank1 pY629 pY671
Cacybp pY200
Cd2ap pY88
Cdc23 pY353
Crk pY108
Ctnnd1 pY96
Dapp1 pY139
Fam120A pY429
Gab2 pY603
Gab3 pY542 pY569
Pag1 pY386
Pik3ap1 pY570
Shank3 pY930
Inppl1 pY1161
Rbck1 pY328
common (552 total sites)
Bcr pY178
Cdk1 pY15 pY19
Cdk17 pY203
Csnk1g1 pY69
Csnk2a1 pY255
Map4k1 pY567
Mapk11 pY182
Mapk12 pY185
Mapk14 pY182
Prkcd pY311 pY332
Rock2 pY722
Btk pY40 pY223 pY344 pY361 pY551
Csk pY18 pY184
Fes pY456
Fyn;Lck pY420;394
Jak2 pY570
Sgk223 pY196
Syk pY202 pY317 pY346
Tec pY518
Tnk2 pY874
Stat6 pY641
Cbl pY672
Cblb pY664 pY763
Cblb;Cbl pY363;369
Trim25 pY277
Pik3ap1 pY694
Pik3cd pY523 pY935
Pik3r1 pY452 pY452 pY467 pY556 pY580 pY657 pY679
Pik3r2 pY458 pY571 pY599
Ppip5k2 pY733
Plcg2 pY371 pY753 pY759 pY1217 pY1245
Inpp5d pY559 pY1021
Inppl1 pY887 pY987 pY1136
Ptpn11 pY62 pY546 pY584
Ptpn6 pY536 pY564
Ptprc pY670
Ptprj pY972
Ubash3a pY9
Ubash3b pY8
Ap2b1 pY737
Cltc pY430 pY634 pY1477
Eps15 pY242
Eps15l1 pY291
Abi1 pY143 pY208
Abi2 pY393
Crkl pY92 pY105 pY251
Dok1 pY361 pY408
Dok2 pY142 pY304 pY402
Dok3 pY343
Gab2 pY263 pY290 pY321 pY632
Grb2 pY209
Hcls1 pY103 pY153 pY175 pY198 pY222 pY323
Memo1 pY210
Nck1 pY105 pY339
Nck2 pY110 pY342
Sh2d3c pY490
Sh2d5 pY177
Shc1 pY423
Skap2 pY75 pY151 pY197 pY260 pY324 pY333
Rasa1 pY451
Was pY214
Wasl pY293
Ywhae pY9 pY214
Ywhag pY216
Ywhah pY216
p190 (106 total sites)
Igf1r pY1167
Jak3 pY781
Lyn, Blk pY193 pY194
Lyn pY306 pY316 pY397 pY473
Peak1 pY528 pY638 pY879
Tnk2 pY40 pY842 pY875
Ptpn18 pY5 pY381
Ptpn11 pY551
Ptpra pY825
Ptpre pY695
Pstpip1 pY344
Ppp1cb pY306
Mtmr10 pY704
Cbl pY698
Dzip3 pY1080
Fam195b pY41
Nfya pY265
F2r pY425
Fcer1g pY76
Mpzl1 pY264
Bub1b pY397
Dyrk1a pY321
Dyrk2 pY380
Gsk3b pY216
Pik3ca pY246
Dok1 pY295 pY314 pY336 pY376 pY397 pY450
Dock11 pY57
Fyb pY559
Itsn2 pY554
Nck2 pY50
Nedd9 pY91 pY165 pY176 pY240 pY260 pY316 pY344
Pag1 pY183 pY314
Pecam1 pY679 pY702
Ppp1r12a pY496
Skap2 pY237
Eps8l2 pY681
kinase activity
phosphatase activity
adapter protein
E3 ubiquitin ligase
clathrin-mediated endocytosis
small GTPase effectors
cytoskeleton-related proteins
transcription regulation
miscellaneous

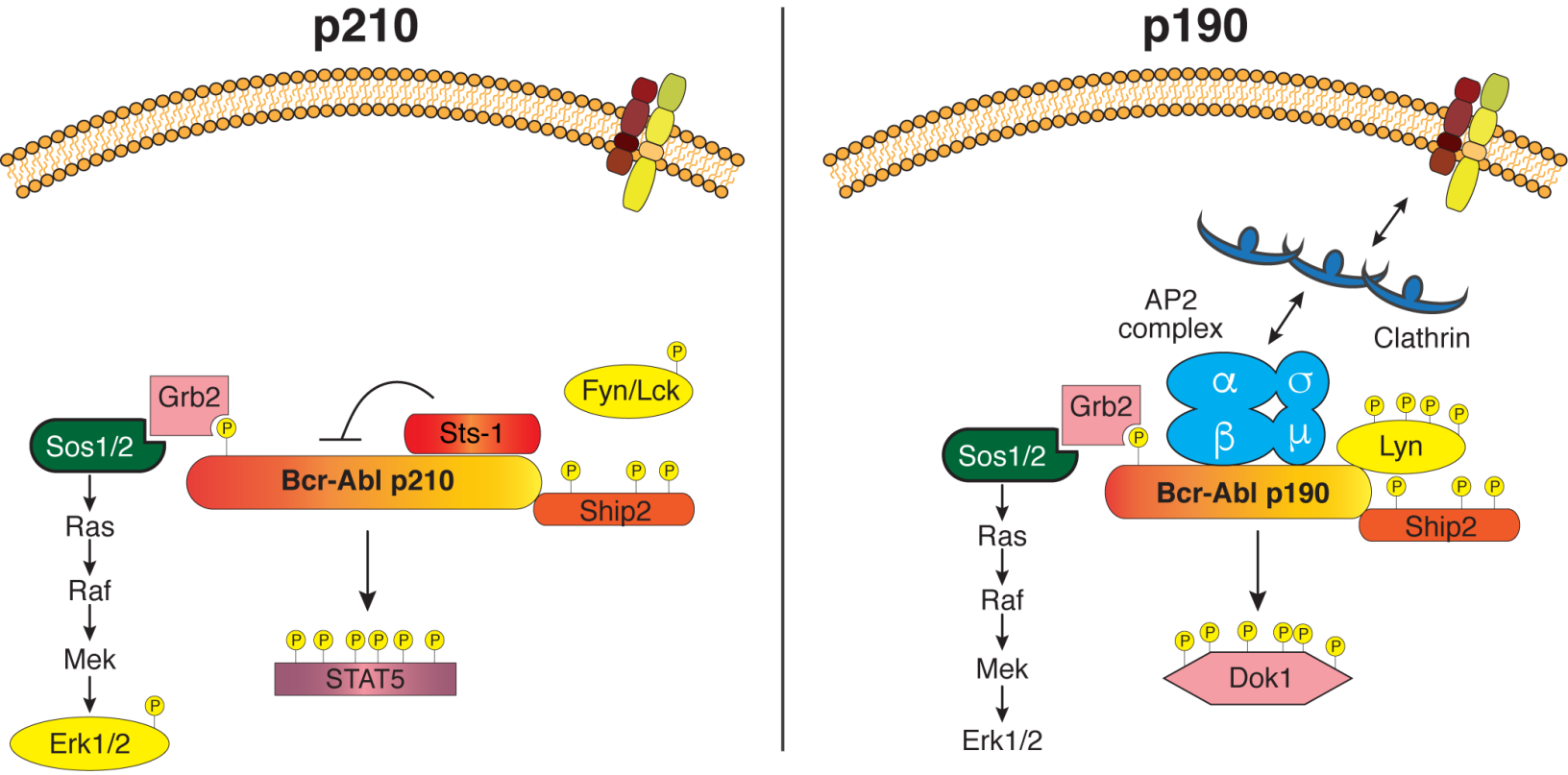
p210
Grb2
Sos1/2
Ras
Raf
Mek
Erk1/2
Fyn/Lck
Sts-1
Bcr-Abl p210
Ship2
STAT5
p190
AP2
complex
Clathrin
α
σ
β
μ
Grb2
Sos1/2
Ras
Raf
Mek
Erk1/2
Lyn
Bcr-Abl p190
Ship2
Dok1